ISME

Numerical Study of the Effect of Materials' Plastic Behavior on Equibiaxial Residual Stress Measurement using Indentation

M.Sanayei[*]
PhD Student

R.Moharami[†]
Associate Professor

Indentation is a new method for estimating residual stress. The plastic behavior of the materials under study can affect indentation parameters and, thus, influences the results of residual stress measurement. In this paper, the effect of yield stress and work-hardening exponent on the accuracy of residual stress measurements in steels and aluminums was studied. Results showed that, for materials with a low strain-hardening exponent and yield strain, Lee's model is applicable; for materials with relatively high amounts of strain-hardening exponent and yield strain, Wang's model is more accurate; and for materials with a medium range of strain-hardening exponent and yield strain all three models can be applied. It was also found that the stresses being tensile or compressive can affect the accuracy of the calculated results for each model. The applicable range of each model is represented in the article.

Keywords: residual stress measurements, indentation, plastic behavior, accuracy.

1 Introduction

Numerous engineering processes (such as shot peening, laser peening, rolling, and grinding) can cause residual stress in components. It is obvious that residual stresses can affect the mechanical behavior of materials, including fracture and fatigue. There are different methods for residual stress measurement, some of which are destructive (e.g. layer removal) and some are nondestructive (e.g. x-ray diffraction). Indentation is a nondestructive method which has widely been used in recent years because of its simplicity of use and applicability on nano- to macro-scales[1]. In (1996), Tsui et al.[2] and Bolshakov et al.[3] studied the relationship between residual stress and material hardness in the indentation test. Affected by these studies, Suresh and Giannakopoulos[4] proposed a model by considering equibiaxial stress state and ignoring pile-up or sink-in effects to measure residual stress. For this purpose, they derived a relationship between the contact areas of indentation with and without the existence of residual stress.
After that, many researchers attempted to develop Suresh and Giannakopoulos's model to accommodate the general state of residual stress and different stress ratios.

[*] PhD Student, University of Zanjan, Department of Mechanical Engineering, m.sanayei@znu.ac.ir
[†] Corresponding Author, Associate Professor, University of Zanjan, Department of Mechanical Engineering, r_moharami@znu.ac.ir

Carlsson and Larsson[5] introduced a new parameter which described the relationship between contact areas and indentation while considering pile-up or sink-in effects. Lee and Kwon[6] modified Suresh's idea and defined residual stress σ_R as the differences between the indentation load with and without stresses on the contact area. Wang et al.[7] developed a model for calculating the residual stress with regard to the indentation work during the indentation process. Bocciarelli and Maier[8] used imprint mapping to identify the bi-dimensional states of stresses. They claimed that the mapped imprint (which, generally, does not exhibit axial-symmetry because of the presence of the residual stress state) directly reflects all the features of bi-dimensional stresses. Then, by applying three-dimensional (3D) simulations and reverse analysis, they proposed a model to measure bi-dimensional residual stress fields. Huber and Heerens[9] and Heerens et al.[10] made a pervasive analysis of the problem by examining how the mechanical properties of the surfaces of the material under investigation are influenced by a residual stress field. It should be noted that Huber and Heerens[9] and Heerens et al.[10] used spherical indentation rather than the sharp indenters utilized by other methods. However, in most studies, sharp indenters are of interest because the hardness and contact area measured by these indenters are independent from indentation depth, which is a particular advantage while explaining the results[11], and also because of the applicability of sharp indenters in non-equibiaxial residual stress fields.
Lee et al.[12] employed numerical approaches with experimental conical indentation. They analyzed the characteristics of conical indentation and selected some normalized parameters which were independent from the indenter's geometry. Afterwards, using dimensional analysis, they presented a model to evaluate general residual stress fields. Lee et al.[13] and Kwon et al.[14] are still developing their model to obtain the general stress field and the ratio of biaxial stresses. Many researchers have also conducted case studies in order to investigate residual stress in particular materials, but their methods are not guaranteed for all materials and occasions. For example, Yonezu et al.[15] proposed a numerical model for estimating the residual stress and pre-strain of austenitic stainless steel by performing a large number of finite-element simulations. Ding and Chromik[16] examined a polycrystalline sample of Fe with nano-indentation and found that texture and strain-hardening can cause differences between stresses on micro- and macro-scales.

Based on these results, they proposed an empirical relationship which demonstrates the potential of predicting macro-scale residual stress levels from nano-indentation experiments. Pham and Kim[17] performed an extensive FE analysis to explore the effects of residual stress and plastic parameters on the indentation response in structural steel. They developed a reverse algorithm to predict unknown parameters (including residual stress, yield stress, and work-hardening exponent) from the indentation test. Their results were in agreement with experiments on SS400 and SM490 steels.

All models represented above need to obtain certain parameters from the indentation test to calculate residual stress fields. These parameters (the contact area between the indenter and the base material, the real amount of indentation depth, pile-up or sink-in of the base material under the indenter, etc.) are affected by the mechanical properties of materials and, if this issue is not considered, it can cause errors in residual stress measurements through indentation.

The purpose of this paper was to study the effect of the yield stress and work-hardening exponent of two widely used material, i.e. steels and aluminums, on the accuracy of residual stress measurement by three commonly used methods, i.e. Suresh's, Lee's, and Wang's models. To this end, numerous finite-element simulations were performed with different values of yield stress, work-hardening exponent, and residual stress fields for both steel and aluminum. For this purpose, a 2D FE model was developed that calculates residual stress using all three models by obtaining P-h curve data.

Then, by comparing the results of the three models with the real amount of applied stresses, it is found which model is suitable for what kind of material; and the applicable range of the three models for steels and aluminums is presented. Previously, a study with this wide range of materials (considering both steels and aluminums) has not been done.

2 Theoretical Background

The schematic diagram of the load-displacement curve for an indenter is shown in Figure (1). The most important data extracted from this chart are: dP/dh, the slope of the initial unloading portion of the P-h curve for the base material; h_c, contact depth (considering pile-up or sink-in); h_r, residual plastic displacement under the indenter after full unloading; and h_{max} and P_{max}, the maximum indentation depth and maximum indentation load, respectively.

Figure (2) depicts two kinds of material responses beneath the indenter: sinking-in which usually occurs in hard metals, and piling-up which is observed in work-hardened (or soft) metals. Of course, different parameters such as the sign of the residual stress field can affect the sinking-in or piling-up of the material[18].

In the following section, a review of the noted models is presented.

2.1 Suresh's Model

Based on Tsui and Bulshakov[2, 3], Suresh et al.[4] assumed that the average contact pressure due to indentation, P_{ave} (and, equivalently, the apparent hardness), is unaffected by any pre-existing tensile or compressive elastic residual stress. Thus, they proposed a model to calculate the residual stress based on the contact pressure and contact area between the Vickers indenter and the base material. To determine the residual stress, they divided the equibiaxial residual stress at the indented surface by a hydrostatic stress plus a uniaxial stress component that causes a differential indentation force, as demonstrated in Figure (3).

Since the differential contact load affects the contact area, Suresh et al. developed the following relation:

$$P_0 - P = f_g . \sigma_R A_c \tag{1}$$

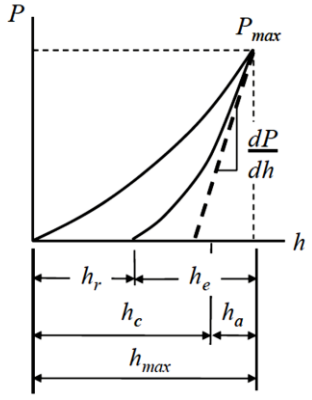

Figure 1 The schematic P-h curve of indentation [19]

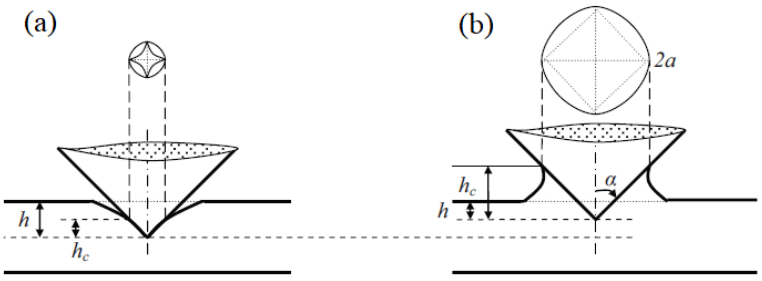

Figure 2 Indentation contact geometry and plan view in the loading condition: (a) Sinking-in, and (b) Piling-up [18]

Where P_0 and P are the maximum loads at the same indentation depth h_{max} with and without residual stress; f_g is a factor which is different in tensile and compressive residual stresses; and A_c is the projected contact area in the stressed sample. By studying the effect of residual stress on the contact area between the indenter and the base material in stress-free and pre-stressed samples, Suresh et al. suggested that the residual stress can be calculated as:

$$\frac{A_{c0}}{A_c} = 1 + \frac{f \cdot \sigma_R}{H} \tag{2}$$

Where A_{c0} represents the projected contact area of the stress-free sample and H denotes the hardness of the stress-free material. f_g is a constant which equals 1 for the tensile residual stress and for the compressive residual stress, $f_g=\sin\theta$, where $\theta = \frac{\pi}{2} - \alpha$ and α is the half angle of the indenter tip.

2.2 Lee's Model

Lee and Kwon[6] developed Suresh et al.'s idea and separated the equibiaxial surface residual stress into mean stress σ_m (hydrostatic stress) and plastic-deformation-sensitive shear deviator stress σ_D:

$$\begin{pmatrix} \sigma_R & 0 & 0 \\ 0 & \sigma_R & 0 \\ 0 & 0 & 0 \end{pmatrix} = \begin{pmatrix} \frac{2}{3}\sigma_R & 0 & 0 \\ 0 & \frac{2}{3}\sigma_R & 0 \\ 0 & 0 & \frac{2}{3}\sigma_R \end{pmatrix} + \begin{pmatrix} \frac{1}{3}\sigma_R & 0 & 0 \\ 0 & \frac{1}{3}\sigma_R & 0 \\ 0 & 0 & -\frac{2}{3}\sigma_R \end{pmatrix} \tag{3}$$

equi-biaxial stress mean stress deviator stress

They assumed that the stress component along the indentation axis in the deviator stress part ($-2\sigma_R/3$) is directly added to the surface-normal indentation pressure. Thus, the difference in the indentation load between stressed and stress-free specimens indented to a specified penetration depth is defined as a residual stress-induced normal load[6]:

$$\sigma_R = \frac{3}{2}\frac{P_0 - P}{A_c} \tag{4}$$

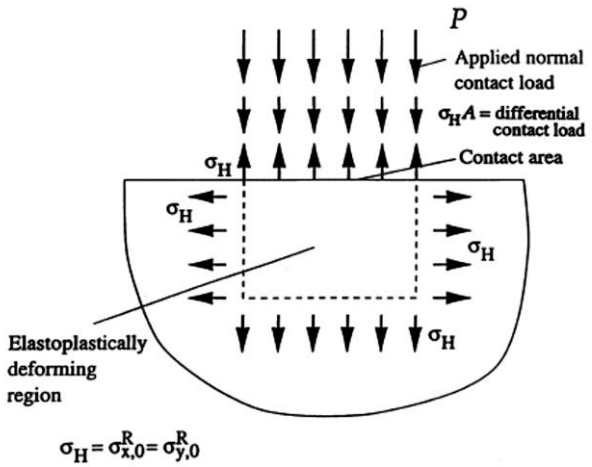

Figure 3 Schematic representation of the role of tensile residual stress on the indented surface [4]

2.3. Wang's Model

Wang et al.[7] used a Berkovich indenter and developed a model to determine residual stress which did not require calculating the contact area between the indenter and the sample's surface. They assumed that the indented surface is subjected to an equibiaxial in-plane residual stress. Based on Suresh's investigations, Wang et al. assumed that, during indentation, elastic responses are completely independent of residual stresses on the indented surface. Therefore, the elastic unloading part of load–depth curves is expected to be unaffected by residual stresses, as shown in Figure (4).

The energy contribution of residual stress can be obtained from the difference between the plastic indentation work U_{OAC} (the plastic indentation work of the stressed sample) and U_{OBC} (the plastic indentation work of the stress-free sample) as:

$$U_{OAB} = U_{OAC} - U_{OBC} = \frac{P - P_0}{3} h_r . \tag{5}$$

in which U_{OAC} and U_{OBC} are the plastic indentation work of stressed and stress-free samples, respectively, and h_r is the residual indentation depth. The energy contribution of residual stresses in an equibiaxial residual stress state can be estimated from the residual indentation impression, as depicted in Figure (4).

$$U_{OAB} = \int_0^{h_r} h \tan\alpha \; \Delta S \, \sigma_R = \int_0^{h_r} h \tan\alpha \left(h \tan\alpha dh \right) \sigma_R = \frac{2}{3} \pi \tan^2 \alpha h_r^3 \sigma_R \tag{6}$$

Where α is the cone semi-angle of the residual indentation impression and can be considered as a geometric correction factor for other sharp indenters. Substituting Equation 6 in Equation 5, the residual stress is calculated as:

$$\sigma_R = \frac{P_0 - P}{2\pi \tan^2 \alpha h_r^2} = \frac{1}{\frac{2h_r^2}{h_c^2}} \cdot \frac{P_0 - P}{A_c} \tag{7}$$

and h_c is the true indentation depth according to the pile-up or sink-in of the sample's surface under indentation.

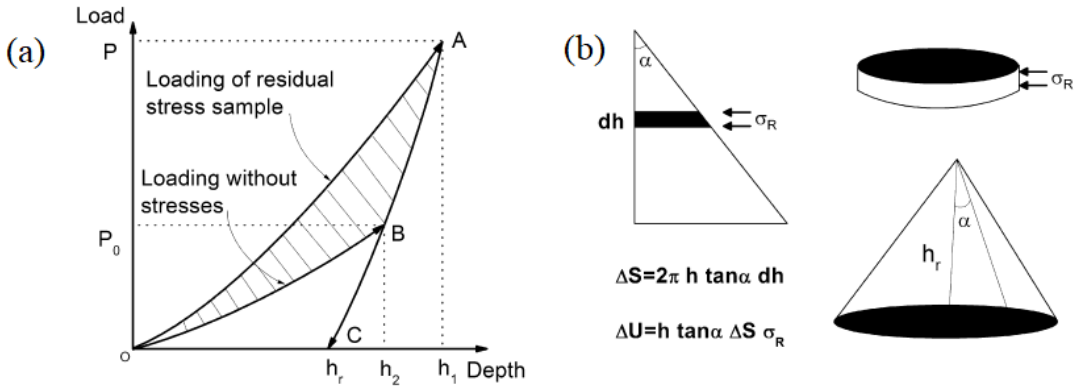

Figure 4 The energy contribution of the residual stress analysis, (a) indentation P–h curves with and without residual stresses, and (b) residual indentation impression after unloading [1]

3 Numerical Analysis

Due to the large number of cases with various combinations of material properties and residual stresses, it is more economical to use numerical analysis instead of empirical experiments. A series of two-dimensional (2D) simulations were performed to explore the effect of work-hardening exponent, yield strain σ_y/E, and different ratios of σ_{res}/σ_y on the accuracy of the residual stress calculated by the three reviewed models. Due to the symmetry of geometry and loading conditions, eight-node axisymmetric elements (CAX8R) were used in the indented body. An analytical rigid conical indenter with a 70.3° half-angle which gave the same area-to-depth ratio as a triangular Berkovich indenter (Wang's model) and a Vickers four-sided pyramid indenter (Suresh's and Lee's models)[20] were utilized. Figure (5) illustrates the schematic representation of the 3D symmetric situations where 2D analyses are acceptable. A typical mesh for the present finite-element simulation is shown in Figure (6-a) with 10000 axisymmetric elements in total which can accurately calculate the results. The investigated body was modeled as a cylinder with 10 mm of height and 10 mm in radius. Boundary conditions are depicted in Figure (6-a). The equibiaxial compressive or tensile stress was applied to the model by applying pressure along the outer surface of the specimen prior to the indentation. The Coulomb friction law was employed between contact surfaces with the friction coefficient of 0.15 [1]. It should be noted that the effect of coulomb friction coefficient on the results of the estimation of residual stresses, both in these simulations and in the previous studies (such as [1,20]), has been carried out, and it has been shown that the Coulomb friction coefficient does not have much effect on the results of residual stress estimation. In all simulations, the penetration depth of the indenter equaled 10 μm. Since a large local deformation occurred directly beneath the indenter, finer meshes were used around the contact region to obtain accurate results, as shown in Figure (6-b). In order to check the independence of simulations from the number of elements, changes in the maximum force at a constant depth of indentation were studied. Figure (7) presents the independence of simulations from the number of elements after the considered 10000 elements.

The base material was modeled as an axisymmetric elastic–plastic von Mises material with an isotropic hardening behavior. The stress–strain relationship of the material is defined as [2121]:

$$\sigma = \begin{cases} E\varepsilon & \varepsilon \le \sigma_y/E \\ R\varepsilon^n & \varepsilon \ge \sigma_y/E \end{cases} \tag{8}$$

in which $R = \sigma_y \left(E/\sigma_y\right)^n$.

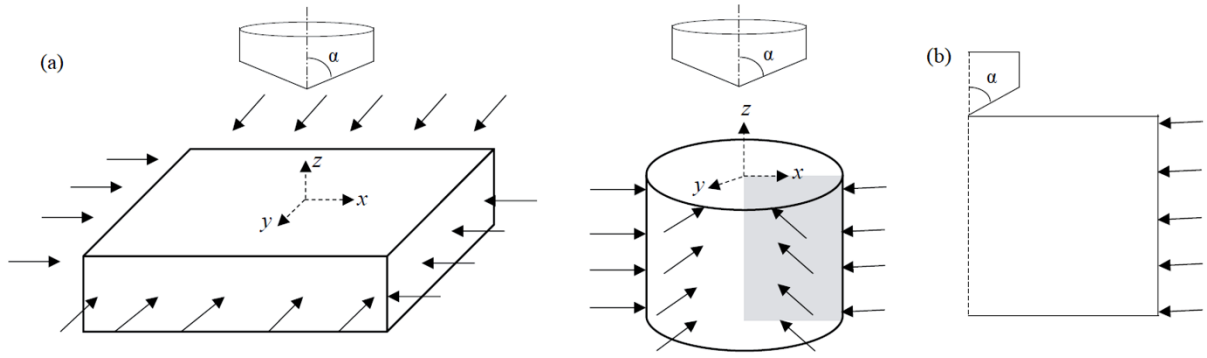

Figure 5 a) A schematic view of 3D symmetric samples with equibiaxial stresses, and b) 2D alternative model

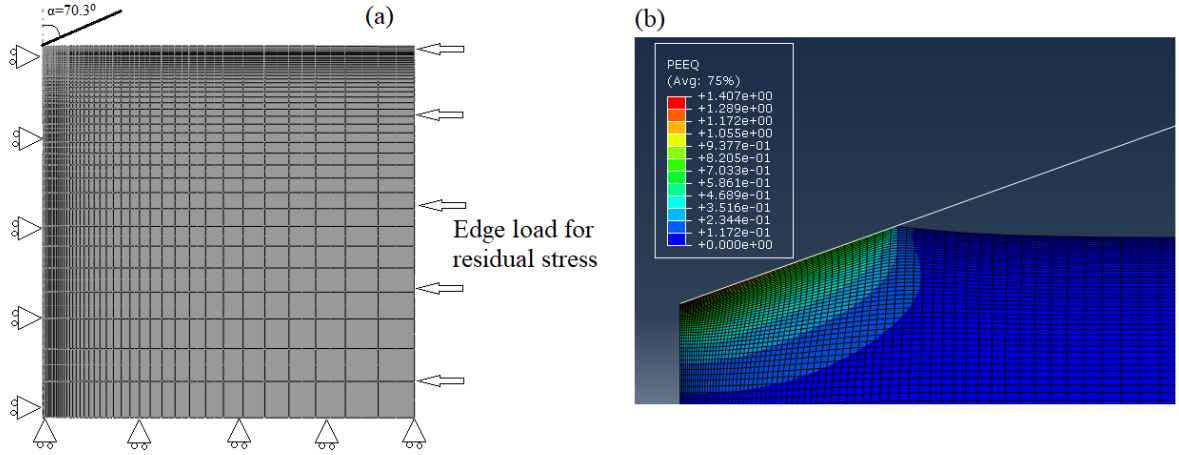

Figure 6 The finite-element model: (a) complete mesh, and (b) denser mesh zones beneath the indenter

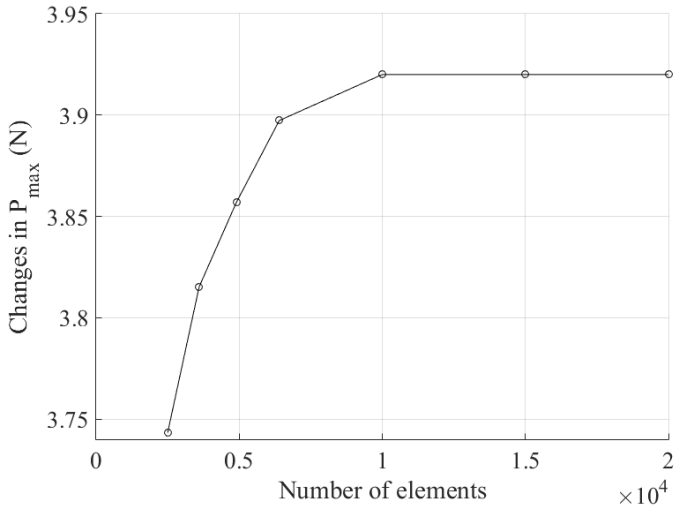

Figure 7 The independence of simulations from the number of elements

A wide range of material property combinations were examined for aluminums and steels by varying residual stress, σ_R, yield strength, σ_y, and work-hardening coefficient, n. For aluminums, Young's modulus equaled 70 GPa for all simulations, yield stress changed from 150 MPa to 250 MPa, and the work-hardening exponent varied from 0.01 to 0.5.

For steels, Young's modulus was 200 GPa for all simulations, yield stress ranged from 250 to 350 MPa, and the work-hardening exponent varied from 0.01 to 0.5. A sample of stress-strain curves of the materials under study is illustrated in Figure (8). The normalized residual stress σ_R/σ_y ranged from -0.8 to 0.8. To take into account all the possible cases, 192 simulations were performed. All studied material properties are listed in Table (1). Figure (9) shows a sample of P-h curves extracted from finite-element simulations for steel with n=0.5 and σ_y/E=0.00125.

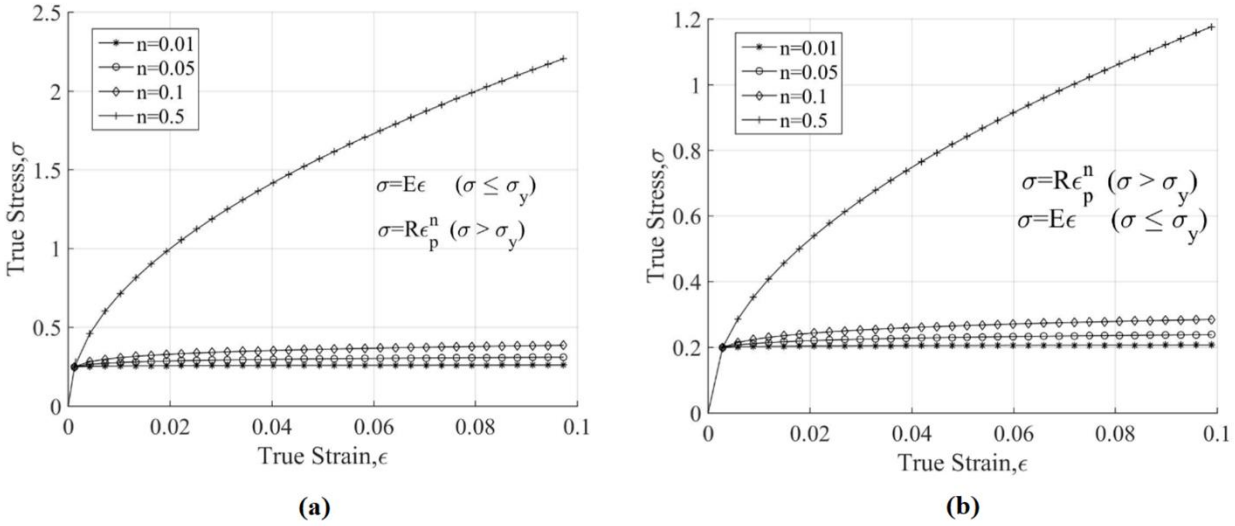

Figure 8 Samples of true stress-true strain curves of materials under study:

a) Steel with σ_y=250MPa, and

b) Aluminum with σ_y=200MPa.

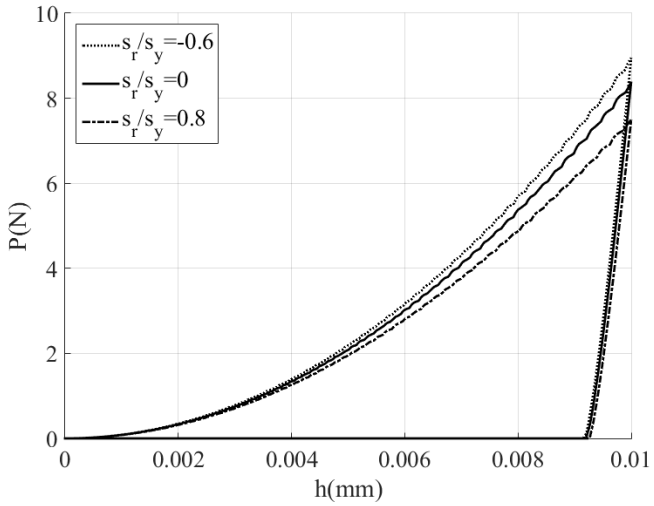

Figure 9 A sample of P-h curves extracted from finite-element simulations for steel with n=0.5 and σ_y/E=0.00125

Table 1 The studied material properties

Material	Young's modulus, E (GPa)	Yield strength, σ_y (MPa)	Work hardening exponent, n	Residual stress ratio, σ_R/σ_y
steel	200	250, 300, 350	0.01, 0.05, 0.1, 0.5	±0.8, ±0.6, ±0.4, ±0.2
aluminum	70	150, 200, 250	0.01, 0.05, 0.1, 0.5	±0.8, ±0.6, ±0.4, ±0.2

4 Results

As mentioned before, the accuracy of the three representative models was obtained in this study by comparing the calculated residual stresses with the applied residual stresses in the FE simulation under four strain-hardening exponents and three yield strains for steels and aluminums. The error of the residual stress calculated by each model in each case was obtained by Equation (9):

$$error = \frac{\sigma_{app} - \sigma_R}{\sigma_{app}} \times 100 \quad (9)$$

A sample of calculated result errors for steel with n=0.05, σ_y=300 MPa, and for aluminum with n=0.1, σ_y=200 MPa, and with different ratios of σ_R/σ_y are represented in Tables (2) and (3), respectively.

Table 2 Typical results of absolute values of error calculations in steel with n=0.05 and σ_y=300 MPa.

σ_R/σ_y	Error of Suresh's Model, %	Error of Lee's Model, %	Errors of Wang's Model, %
-0.8	24.4	29.9	65.9
-0.6	2.9	41.9	71.7
-0.4	30.4	25.9	63.9
-0.2	42.7	64.3	82.6
+0.2	29.4	19.8	41.8
+0.4	39.6	14.5	44.4
+0.6	45.3	2.7	50.2
+0.8	41.1	11.7	45.9

Table 3 typical results of absolute values of error calculations in aluminum with n=0.05 and σ_y=200 MPa.

σ_R/σ_y	Error of Suresh's Model, %	Error of Lee's Model, %	Errors of Wang's Model, %
-0.8	117.6	21.5	40.1
-0.6	102.9	16.4	42.7
-0.4	138.3	22.8	39.4
-0.2	163.0	43.4	29.5
+0.2	14.8	50.4	26.3
+0.4	18.4	52.4	25.5
+0.6	21.4	53.3	25.1
+0.8	25.8	56.4	23.7

5 Discussions

Figure (10) shows some typical results for steel cases, and Figure (11) illustrates the cases of aluminum. In these figures, both calculated residual stresses (σ_R) and applied stresses (σ_{app}) are normalized by yield stress (σ_y) and the dashed line is the ideal situation where the calculated residual stress is equal to the applied stress.

Figures (10-a) to (10-d) demonstrates the results of steels with different strain-hardening exponents at the same yield strain $\sigma_y/E = 0.0015$. For steels with small strain-hardening exponents (n=0.01 and n=0.05), Lee's model had the best answers in tensile residual stresses and Suresh's model had more precise predictions for compressive residual stresses.

Figure (10-c) indicates the results of the three models for n=0.1. In both tensile and compressive residual stresses, the results predicted by Lee's model were the most accurate. In this case, Wang's model underestimated the amount of applied stress, while Suresh's model overestimated the results in compressive and underestimated them in tensile residual stresses.

In steels with relatively high strain-hardening exponents (n=0.5), such as the one illustrated in Figure (10-d), Wang's model had the most accurate predictions. Both Lee's and Suresh's estimations seriously deviated from the applied residual stresses, especially in compressive stresses.

Figures (10-c), (10-e), and (10-f) compare the results at different yield strains with the same strain-hardening exponent n = 0.1. It seems that, in lower amounts of yield strain, the predictions by Lee's model predictions were more compatible with the applied stresses. In higher amounts of yield strain, Lee's model had good answers only in the compressive stress state, but in tensile residual stresses, Wang's and Suresh's model were more precise. In general, yield strain does not seem to be as effective as the strain-hardening exponent on the accuracy of predicted residual stresses.

The same analysis procedure was applicable for aluminum. Figure (11-a) to (11-d) shows the results of aluminums with different strain-hardening exponents at the same yield strain $\sigma_y/E = 0.0029$. In the case of aluminums with small or medium strain-hardening exponents (n=0.01, 0.05, and 0.1), the predictions by Lee's model were in good agreement with the applied compressive stresses, while in the tensile residual stress state, Wang's and Suresh's models were more accurate. For aluminums with relatively high strain-hardening exponents (n=0.5), the answers of Wang model were very precise, while the other two models highly overestimated the amount of applied stress, especially in the compressive state.

Figures (11-c), (11-e), and (11-f) compare the results at various yield strains with the same strain-hardening exponent n = 0.1 for aluminum. At lower ranges of yield strain, Lee's model had the most accurate predictions of the amount of residual stress. As the yield strain increased, Lee's model was applicable only in compressive stresses. The answers of Wang's model seemed suitable for relatively high-strain-hardening materials. For aluminums with medium yield strains, Wang's and Suresh's model were more precise in predicting the tensile residual stress. However, for the compressive stress state, Lee's model had the best answers. Also, Suresh's model made a good prediction of tensile stress amount in aluminums with high strain-hardening exponents.

A summary of the results is presented in tables (4) and (5).

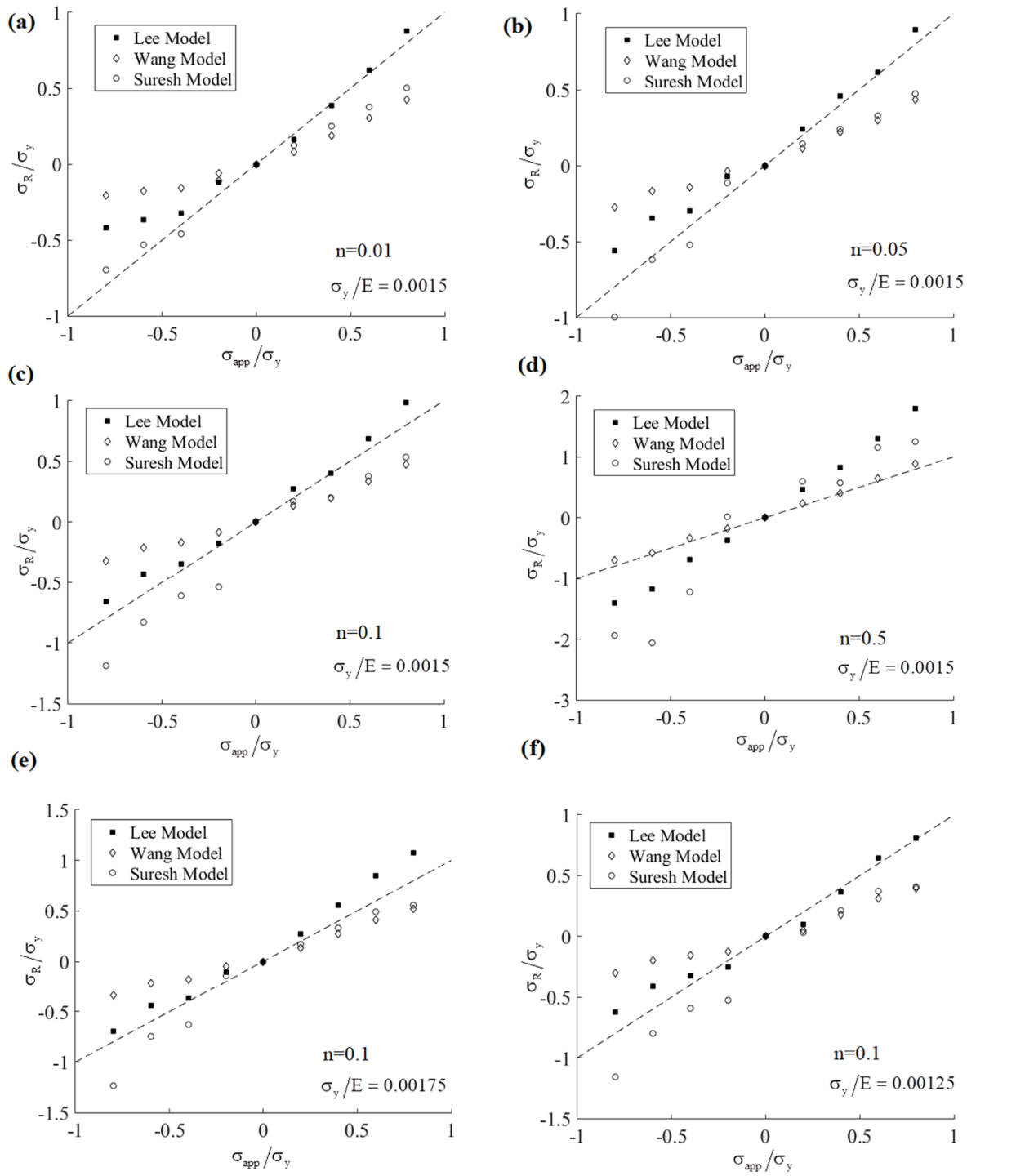

Figure 10 A comparison of the calculated residual stresses with the applied stresses at different strain-hardening exponents and different yield strains for steel: a) n=0.01, E/σ_y=0.0015; b) n=0.05, E/σ_y=0.0015; c) n=0.1, E/σ_y=0.0015; d) n=0.5, E/σ_y=0.0015; e) n=0.1, E/σ_y=0.00125; f) n=0.1, E/σ_y=0.00175

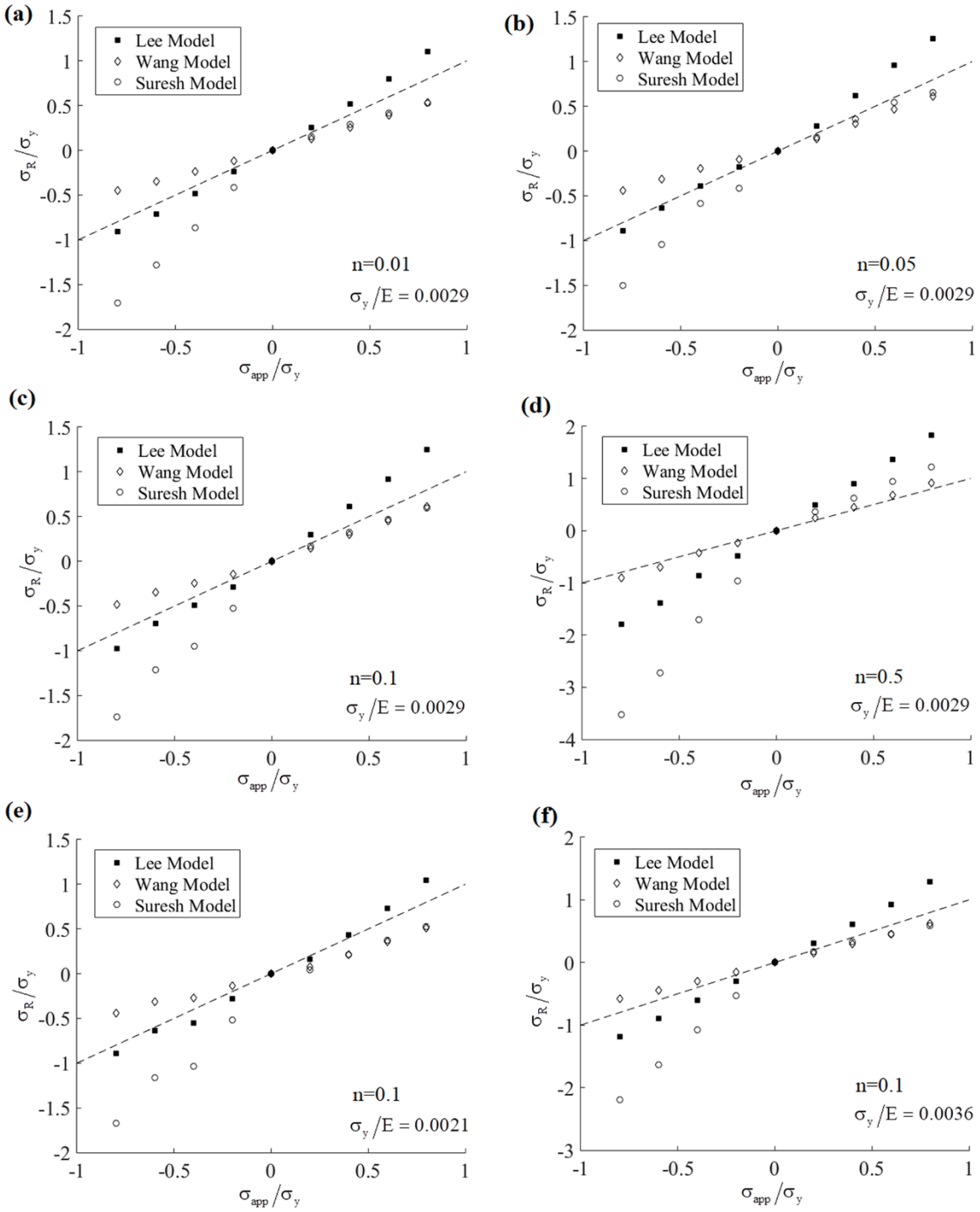

Figure 11 A comparison of the calculated residual stresses with the applied stresses at different strain hardening exponents and different yield strains for aluminum: a) n=0.01, E/σ_y=0.0029; b) n=0.05, E/σ_y=0.0029; c) n=0.1, E/σ_y=0.0029; d) n=0.5, E/σ_y=0.0029; e) n=0.1, E/σ_y=0.0021; f) n=0.1, E/σ_y=0.0036

Table 4 Applicable range of each model in steel

The state of residual stress	Lee's Model	Suresh's Model	Wang's Model
Tensile	$0.01 \le n \le 0.1$	$n = 0.01$	$n = 0.5$
Compressive	$n = 0.1$	$0.01 \le n \le 0.05$	$n = 0.5$

Table 5 Applicable range of each model in aluminum

The state of residual stress	Lee's Model	Suresh's Model	Wang's Model
Tensile	$n = 0.01$	$0.01 \le n \le 0.1$	$0.01 \le n \le 0.5$
Compressive	$0.01 \le n \le 0.1$	$n = 0.01$	$n = 0.5$

6 Conclusion

In this paper, three models, i.e. Suresh's model, Lee's model, and Wang's model, were reviewed for residual stress calculation through indentation. Afterwards, using finite-element simulations, the effect of materials' yield strength, σ_y, and strain-hardening exponent, n, on the accuracy of each model's predictions were studied. It was found that, in steels, for materials with low strain-hardening exponents, Lee's model is suitable for tensile stresses and Suresh's model is good for the compressive stress state. Lee's model is also applicable for materials with medium hardening exponents. Nevertheless, for materials with high strain-hardening exponents, Wang's model has the most accurate answers.

In aluminums, it was found that, in materials with small or medium strain-hardening exponents, the predictions by Lee's model are in good agreement with the applied compressive stresses. However, in the tensile residual stress state, Wang's and Suresh's models are more accurate. For aluminums with relatively high strain-hardening exponents, the answers of Wang model are very precise.

Examining the effects of yield strain on the three models showed that Lee's model is more accurate in small yield strains and Wang's model has the best answers for materials with high yield strains. For materials with medium yield strains, Lee's model is applicable for compressive residual stresses and Wang's and Suresh's models are good for the tensile stress state.

References

[1] Xiao, L., Ye, D., and Chen, C., "A Further Study on Representative Models for Calculating the Residual Stress Based on the Instrumented Indentation Technique", Comp. Mater. Sci. Vol. 82, pp. 476-482, (2014).

[2] Tsui, T.Y., Oliver ,W.C., and Pharr, G.M., "Influences of Stress on the Measurement of Mechanical Properties using Nanoindentation: Part I. Experimental Studies in an Aluminum Alloy", J. Mater. Research, Vol. 11, No. 03, pp. 752-759, (1996).

[3] Bolshakov, A., Oliver ,W.C., and Pharr, G.M., "Influences of Stress on the Measurement of Mechanical Properties using Nanoindentation: Part II. Finite Element Simulations", J. Mater. Research, Vol. 11, No. 03, pp. 760-768, (1996).

[4] Suresh, S., and Giannakopoulos, A.E., "A New Method for Estimating Residual Stresses by Instrumented Sharp Indentation", Acta Mater. Vol. 46, No. 16, pp. 5755-5767, (1998).

[5] Carlsson, S., and Larsson, P.L., "On the Determination of Residual Stress and Strain Fields by Sharp Indentation Testing.: Part I: Theoretical and Numerical Analysis", Acta Mater. Vol. 49, No. 12, pp. 2179-2191, (2001).

[6] Lee, Y.H., and Kwon, D., "Measurement of Residual-stress Effect by Nanoindentation on Elastically Strained (1 0 0) W", Scripta Mater. Vol. 49, No. 5, pp. 459-465, (2003).

[7] Wang, Q., Ozaki, K., Ishikawa, H., Nakano, S., and Ogiso, H., "Indentation Method to Measure the Residual Stress Induced by Ion Implantation", Nucl. Instrum. Methods Phys. Res. B, Vol. 242, No. 1–2, pp. 88-92, (2006).

[8] Bocciarelli, M., and Maier, G., "Indentation and Imprint Mapping Method for Identification of Residual Stresses", Comp. Mater. Sci. Vol. 39, No. 2, pp. 381-392, (2007).

[9] Huber, N., and Heerens, J., "On the Effect of a General Residual Stress State on Indentation and Hardness Testing", Acta Mater. Vol. 56, No. 20, pp. 6205-6213, (2008).

[10] Heerens, J., Mubarok, F., and Huber, N., "Influence of Specimen Preparation, Microstructure Anisotropy, and Residual Stresses on Stress–strain Curves of Rolled Al2024 T351 as Derived from Spherical Indentation Tests", J. Mater. Research,Vol. 24, No. 3, pp. 907-917, (2011).

[11] Rydin, A., and Larsson, P.L., "On the Correlation between Residual Stresses and Global Indentation Quantities: Equi-Biaxial Stress Field", Tribol. Lett. Vol. 47, No. 1, pp. 31-42, (2012).

[12] Lee, J.H., Lee, H., Hyun, H.C., and Kim, M., "Numerical Approaches and Experimental Verification of the Conical Indentation Techniques for Residual Stress Evaluation", J. Mater. Research, Vol. 25, No. 11, pp. 2212-2223, (2011).

[13] Rickhey, F., Lee, J.H., and Lee, H., "A Contact Size-independent Approach to the Estimation of Biaxial Residual Stresses by Knoop Indentation", Mater. Des., Vol. 84, pp. 300-312, (2015).

[14] Ahn, H.J., Kim, J.h., Xu, H., Lee, J., Kim, J.Y., Kim, Y.C., and Kwon, D., "Directionality of Residual Stress Evaluated by Instrumented Indentation Testing using Wedge Indenter", Met. Mater. Int., Vol. 23, No. 3, pp. 465-472, (2017).

[15] Yonezu, A., Kusano, R., Hiyoshi, T., and Chen, X., "A Method to Estimate Residual Stress in Austenitic Stainless Steel using a Microindentation Test", J. Mater. Eng. Perform. Vol. 24, No. 1, pp. 362-372, (2015).

[16] Ding, Y., and Chromik, R.R., "Relationship between Indentation Plastic Zone Size and Residual Stresses in Plastically Deformed Fe", Mater. Sci. Eng A Struct. Mater. Vol. 696, pp. 1-9, (2017).

[17] Pham, T.H., and Kim, S.E., "Determination of Equi-biaxial Residual Stress and Plastic Properties in Structural Steel using Instrumented Indentation", Mater. Sci. Eng. Struct. Mater(A). Vol. 688, pp. 352-363, (2017).

[18] H Faisal, N., and Ahmed, R., "A Review of Patented Methodologies in Instrumented Indentation Residual Stress Measurements", Recent Pat. Mech. Eng. Vol. 4, No. 2, pp. 138-152, (2011).

[19] Fischer-Cripps, A., "*Nanoindentation*", Springer, New York, pp. 21-37, (2011).

[20] Fischer-Cripps, A.C., "*Nanoindentation*", Springer, New York, pp. 105-117, (2011)

[21] Yan, J., Karlsson, A.M., and Chen, X., "Determining Plastic Properties of a Material with Residual Stress by using Conical Indentation", Int. J. Solids Struct. Vol. 44, No. 11, pp. 3720-3737, (2007).

Nomenclature

This list is located before the list of references and should include English symbols followed by Greek symbols in alphabetical order as the following examples:

A_c Real projected contact area between the indenter and the specimen, m^2

A *P*rojected contact area between the indenter and the specimen, m^2

E Modulus of elasticity, N/m^2

P Force, N

h Displacement of the indenter during indentation, m

dp/dh The slope of the initial unloading portion of the P-h curve, N/m

h_c The real contact depth, m

h_r Residual plastic displacement under the indenter after full unloading, m

σ_R Residual stress, N/m^2

σ_y Yield stress, N/m^2

n Work hardening exponent

Greek symbols

ε Strain

چکیده

استفاده از آزمون فرورونده، روشی نوین برای اندازه‌گیری تنش پسماند است. رفتار پلاستیک ماده‌ی تحت بررسی می‌تواند پارامترهای آزمون، و در نتیجه، نتایج اندازه‌گیری تنش پسماند را تحت تاثیر قرار دهد. در این مقاله، اثر تنش تسلیم و توان کرنش‌سختی بر روی دقت اندازه‌گیری تنش پشماند در فولادها و آلومینیوم‌ها با استفاده از سه مدل رایج لی، سورش و وانگ، مورد مطالعه قرار گرفته است.

نتایج نشان می‌دهند که برای مواد با توان کرنش‌سختی و کرنش تسلیم کم، مدل لی قابل اعمال است؛ برای مواد با مقادیر نسبتاً زیاد توان کرنش‌سختی و کرنش تسلیم، مدل وانگ جواب‌های دقیق‌تری دارد؛ و برای موادی که کرنش تسلیم و توان کرنش‌سختی آن‌ها مقدار متوسطی دارد، از هر سه مدل بررسی شده در این مقاله می‌توان استفاده کرد. همچنین مشخص شد که کششی یا فشاری بودن تنش‌های پسماند، می‌تواند بر دقت نتایج محاسبه شده در هر مدل تاثیر بگذارد. بازه‌ای که در آن هر یک از مدل‌ها قابل استفاده است در مقاله ارائه شده است.